Nuclear Inst. and Methods in Physics Research, A 958 (2020) 162127

Contents lists available at ScienceDirect

Nuclear Inst. and Methods in Physics Research, A

journal homepage: www.elsevier.com/locate/nima

The Gigatracker, the silicon beam tracker for the NA62 experiment at CERN

L. Federici [a,*], G. Aglieri Rinella [a], D. Alvarez Feito [a], R. Arcidiacono [b,c], C. Biino [b], S. Bonacini [a], A. Ceccucci [a], S. Chiozzi [d], E. Cortina Gil [e], A. Cotta Ramusino [d], J. Degrange [a], M. Fiorini [d], E. Gamberini [a], A. Gianoli [d], J. Kaplon [a], A. Kleimenova [e], A. Kluge [a], A. Mapelli [a], F. Marchetto [b], E. Migliore [b], E. Minucci [e], M. Morel [a], J. Noël [a], M. Noy [a], L. Perktold [a], M. Perrin-Terrin [f], P. Petagna [a], F. Petrucci [d], K. Poltorak [a], G. Romagnoli [a], G. Ruggiero [g], B. Velghe [e], H. Wahl [d]

[a] *CERN, Geneva, Switzerland*
[b] *INFN Sezione di Torino and University of Torino, Torino, Italy*
[c] *Univesità degli studi del Piemonte Orientale, Vercelli, Italy*
[d] *INFN Sezione di Ferrara and University of Ferrara, Ferrara, Italy*
[e] *Université Catholique de Louvain, Louvain-la-Neuve, Belgium*
[f] *Aix Marseille Univ., CNRS/IN2P3, CPPM, Marseille, France*
[g] *Lancaster University, Lancaster, UK*

A R T I C L E I N F O

MSC:
00-01
99-00

Keywords:
Tracking detector
Silicon detector
Hybrid silicon detector
Pixel detector
Micro-channels cooling
Time resolution
Material budget
Gigatracker
GTK
NA62

A B S T R A C T

The Gigatracker is the NA62 beam tracker. It is made of three $63.1\,mm \times 29.3\,mm$ stations of $300\,\mu m \times 300\,\mu m$ hybrid silicon pixel detectors installed in vacuum ($\sim 10^{-6}\,mbar$). The beam particles, flowing at $750\,MHz$, are traced in 4-dimensions by mean of time-stamping pixels with a design resolution of $200\,ps$. This performance has to be maintained despite the beam irradiation amounting to a yearly fluence of 2×10^{14} 1 MeV n_{eq}/cm^2. The detector material minimization is paramount, as the detector faces the full beam. The station material budget is reduced to $0.5\%\,X_0$ by using (HEP world first) micro-channels cooling. We will describe the detector design and performances during the NA62 runs.

1. Introduction

The NA62 experiment. The NA62 experiment at CERN SPS started to collect data in 2016 in order to settle the new precision limit of 10% in the $\mathcal{B}(K^+ \to \pi^+ \nu\bar{\nu})$ measurement, pushing forward the experimental test of the Standard Model (SM) prediction:

$$\mathcal{B}(K^+ \to \pi^+ \nu\bar{\nu}) = (8.4 \pm 1) \times 10^{-11}$$

The experiment main strategy stands on the use of a decay-in-flight technique to detect the daughter particles produced by the K^+ decay in the appointed 60 m long decay region starting 102.4 m downstream of a 40 cm long Beryllium target. The 400 GeV primary beam extracted from the SPS ring is set up for a more efficient detection and identification of the Kaon's decay products. The 75 GeV secondary beam emerging from the fixed target has a nominal rate of 750 MHz and only 6% of it are K^+. A detailed description of the NA62 experiment can be found in [1]. See Fig. 1 for a schematic view of the NA62 experiment.

The detector role and experiment constraints. In the measurement of an ultra-rare decay the main challenging aspect is to separate the signal (the $K^+ \to \pi^+ \nu\bar{\nu}$) from the backgrounds. In particular the resolution on the detection of $K^+ \to \pi^+ \pi^0$ squared missing mass leads to stringent conditions in the angular ($p_{x,y}/p_z = 16\,\mu rad$) and momentum ($\delta p/p = 0.2\%$) resolution of the beam particles. The charged particles beam goes through the three detector's modules. Therefore the reduction of the inelastic scattering probability, by limiting the maximum material budget the detector can expose to the beam, is mandatory. A limit of $1.5\%\,X_0$ for the entire detector is required. Moreover, in order to unambiguously associate a track with outcomes from other detectors, the detector has to ensure a hit time resolution better than 200 ps. All

* Corresponding author.
E-mail address: lfederic@cern.ch (L. Federici).

https://doi.org/10.1016/j.nima.2019.04.081
Received 31 March 2019; Received in revised form 18 April 2019; Accepted 23 April 2019
Available online 27 April 2019

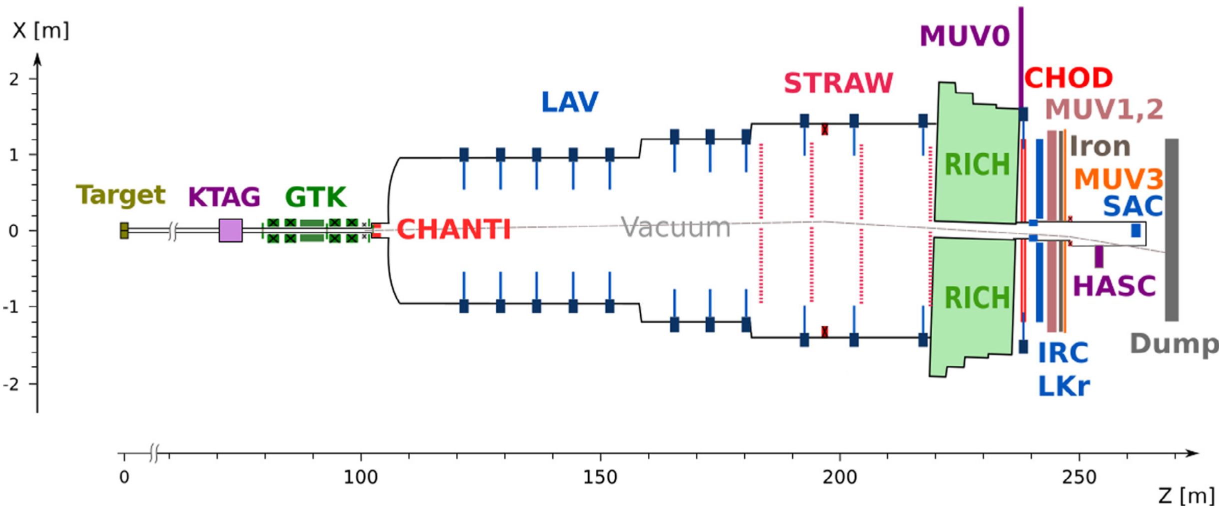

Fig. 1. A schematic of the sub-detectors position in the NA62 experimental area. The Gigatracker is placed between the Cherenkov detector for the Kaon identification (KTAG) and the detector for the particles produced by the inelastic scattering with the third GTK station (CHANTI), just before the beginning of the Kaon decay fiducial volume.

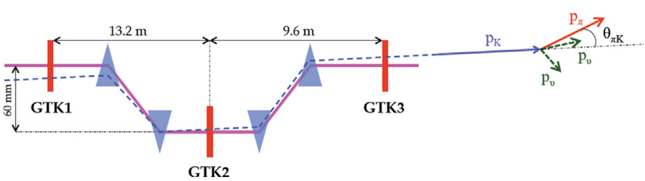

Fig. 2. A (X,Z) schematic of the three GTK stations installation configuration in the experimental area. The particle direction is measured by the position detected in the GTK1 and GTK3. The particle momentum, related to the vertical displacement undergone in the magnet pairs, is obtained including the position measured on GTK2.

these constraints must be satisfied taking in consideration the expected average particles rate of 750 MHz (with fluctuations up to 1 GHz and a peak rate of 1.5 MHz/mm^2 in the center of the detector area) and a fluence of 2×10^{14} 1 MeV n$_{eq}$/cm^2 per average data taking period per year (∼ 100 days). The Gigatracker (GTK) was designed and built to fulfill this goal.

2. The Gigatracker

The GTK is the hybrid pixel silicon beam spectrometer of the NA62 experiment. It is made of three identical and independent stations interleaved with two pairs of bending magnets (as shown in Fig. 2) to measure the momentum of the particles passing through the three sensitive parts of the detector. An individual GTK station is made of: a detector module, an high and low voltage power supply, an interlock module, a set of 10 DAQ boards and 2 DAQ PCs. In the following a brief description of the detector modules components:

The GTK hybrid. The sensitive part of the detector is a 200 μm thick (0.2% X_0) n-on-p Si sensor with an area of 27.0×60.8 mm^2. Its thickness is the result of the trade-off between the requested material budget and the endurance to radiation damages preserving at the same time the capability to provide enough signal (15×10^3 e-h pairs) per incoming 75 GeV/c particle. During the data taking the sensor was polarized with V_{bias} = 100 V.

The sensor is read out by 10 12×20.37 mm^2 custom ASICs, the TDCPix [2–6], built with the 130 nm IBM technology. Each TDCPix (Fig. 4) is made of two separated areas: the analog 40×45 pixel matrix (300×300 μm^2 pixel size), bump bonded to the sensor (Fig. 3), where the hit signals are digitized and the End-Of-Column (EOC) where a time stamp is assigned to those signals before their serialization for the transmission out of the chip. The signal generated at the pixel level is shipped via a dedicated transmission line to the EOC area where a time stamp, evaluated on the hit signal leading and trailing edges, is assigned to the hit by two Time to Digital Converters (TDC). The number of required TDC channels is reduced multiplexing the 45 pixels of one column into 9 groups of 5 pixels using an asynchronous multiplexer circuit (hitArbiter) located in the EOC region. The time information is delivered with a 100 ps binning. The hit pixel address together with its assigned time stamp are encoded in a 48 bits word ready to be sent out of the chip via one of the 4 3.2 GHz serializers, each one serving a set of 10 pixels matrix columns. The TDCPix will operate in a high radiation environment therefore a Triple Modular Redundancy (TMR) has been implemented on the logic controlling the TDC data flow in order to protect against Single Event Upset (SEU) effects. Before connecting to the sensor, each TDCPix is thinned down to 100 μm (0.1% X_0) to fulfill the material budget constrain. Since the power consumption per chip is ∼ 4 W, mainly due to the EOC, an active cooling system is imperative.

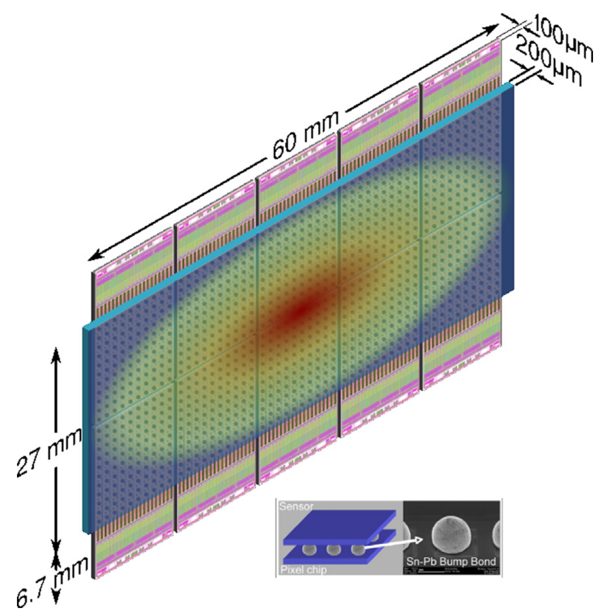

Fig. 3. The 200 μm thick sensor is bump bonded to the 10 pixel matrices of the 2×5 TDCPixes configuration by mean of 1800 30 μm SnPb bump bonds to form the GTK hybrid.

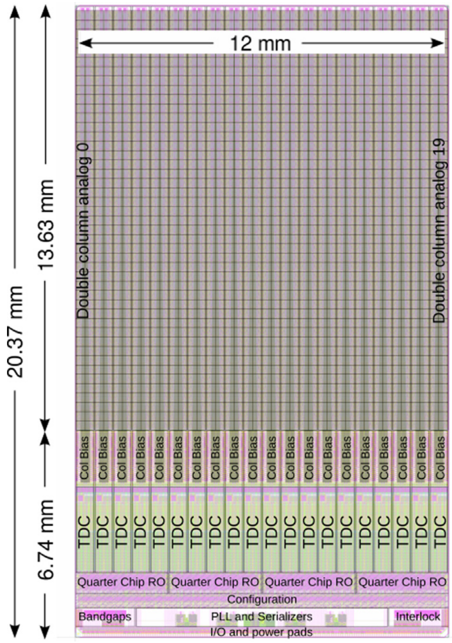

Fig. 4. The TDCPix is the custom ASIC realized to read out the Si Sensor of the GTK. It is made of two separated areas: the 1800 pixels matrix (each pixel occupying an area of $300 \times 300\,\mu\mathrm{m}^2$) ($13.63 \times 12\,\mathrm{mm}^2$, the top part in the figure) where the hit signal is digitized and the End-Of-Column area ($6.74 \times 12\,\mathrm{mm}^2$, the bottom part in the figure) where the hit time is measured and the 48 bits output word is built. The TDCPix contains 1800 front-end circuits including 1800 threshold trim DACs, 40 column DACs, 1800 transmission drivers/receivers/lines, 360 hitArbiters, 720 TDC channels with 20 DLLs, 4 read-out controllers, 4 serializers, 4 parallel output ports.

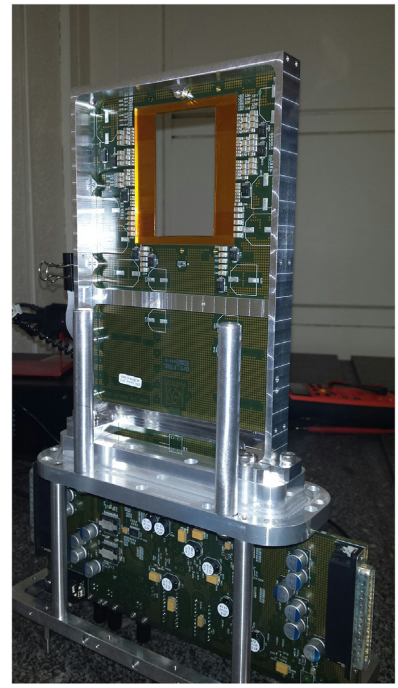

Fig. 5. The GTK assembly Carrier PCB placed vertically. The bottom part, delimited by the horizontal aluminum flange, stands out of the vacuum vessel and holds the power and optical components while at the top, in vacuum, the countersink holds the GTK assembly (not present in the picture) wire bonded to the board. The integrity of the high speed signals ($40 \times 3.2\,\mathrm{GHz}$) on a such long distance is guaranteed by using the ISOLA FR408 material for the PCB.

The GTK assembly. The GTK is the first detector in HEP to employ a micro-channels (μ-channels) cooling plate [7] to control its temperature while operating in the vacuum. The cooling plate is fabricated directly in a Si wafer were the 150 $200 \times 70\,\mu\mathrm{m}^2$ μ-channels are etched. The thickness in the area matching the detector acceptance is reduced to $210\,\mu\mathrm{m}$ ($0.2\%\ X_0$). The cooling plate is glued to the GTK hybrid by mean of the 3M 9461P100 tape and the liquid coolant C_6F_{14} flows at $3\,\mathrm{g/s}$ in the μ-channels keeping the sensor and the front-end electronics at $-10°C$ while fully operational (see the cooling side view of a complete GTK module in Fig. 8).

The GTK assembly carrier. The GTK assembly carrier is a 14 layers PCB board fully integrated with a vacuum flange and aluminum frame forming the only vacuum feedthrough of the module. The high speed ($3.2\,\mathrm{GHz}$) signals must be delivered from the TDCPixes, in vacuum, to the optical links outside the vacuum vessel. In order to ensure their integrity the PCB board is produced with the ISOLA FR408 epoxy laminate and prepreg [8]. The GTK assembly is housed in the countersink, a machined area in the vacuum side of the board (see Fig. 5), where the GTK hybrid can be electrically connected via 1430 wire bonds with $75\,\mu\mathrm{m}$ pitch to the carrier PCB.

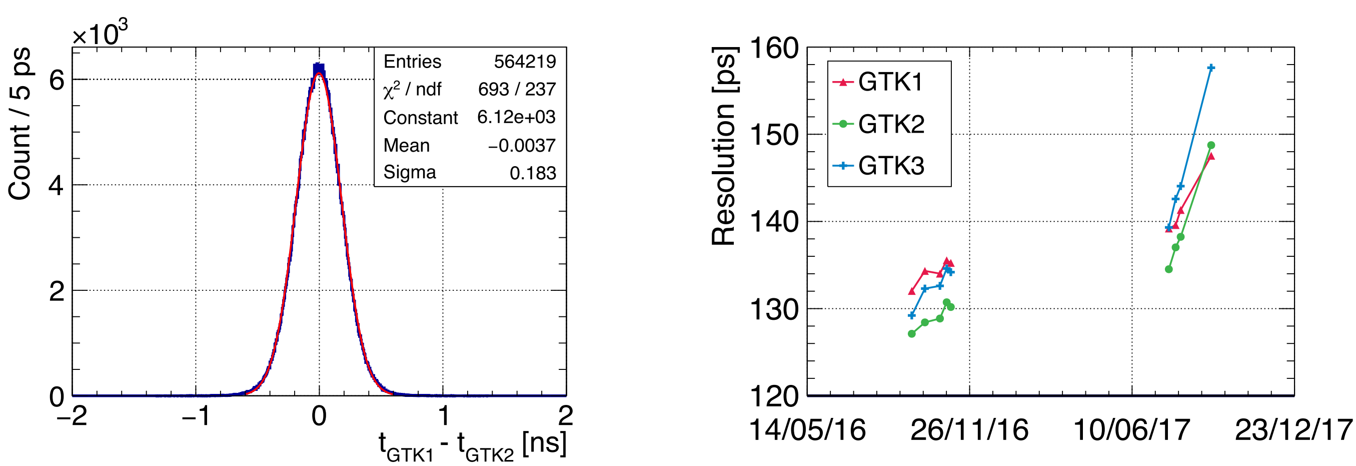

(a) (b)

Fig. 6. (a) A standalone measurement of the time resolution is obtained comparing the hit time difference among the three stations for the same K^+ event (between the station 1 and 2 in this example). The time resolution values obtained are: $\Delta t_{GTK1} = 132.0\,\mathrm{ps}$, $\Delta t_{GTK2} = 127.1\,\mathrm{ps}$, $\Delta t_{GTK3} = 129.2\,\mathrm{ps}$. (b) The time resolution degrades over time due to the charged particle fluence (0.26×10^{14} 1 MeV $\mathrm{n_{eq}/cm^2}$ in the shown time period), but it is still better than then nominal specifications. The empty space in the middle of the dataset represent the annual winter stop period when the installed three modules were stored at -21 °C.

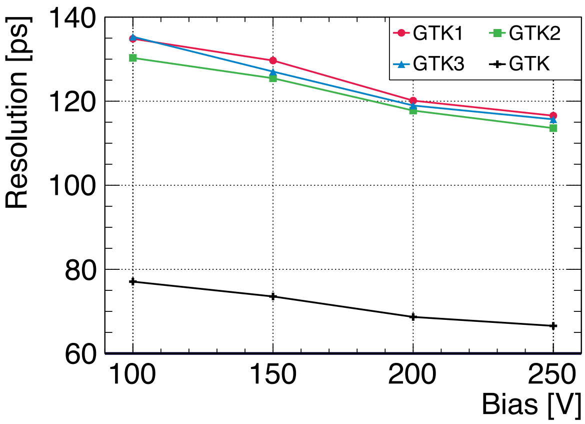

Fig. 7. The trend of the time resolution as function of the bias voltage applied to the sensor measured at experiment conditions. The top lines are the trends of the individual station while the bottom line is the time resolution obtained combining the individual measurement on the three stations.

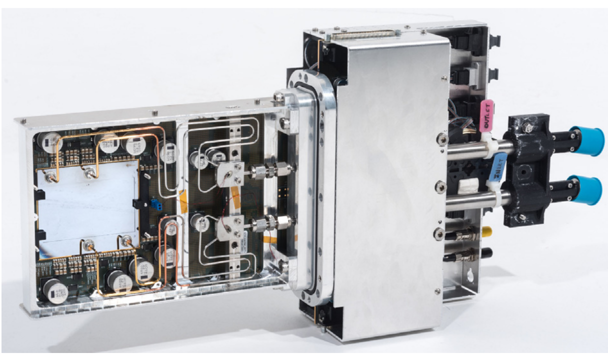

Fig. 8. A complete GTK module shown on the cooling system side. On the right (blue caps) the inlet (bottom) and outlet (top) through which the coolant C_6F_{14} flows. The coolant reaches the μ-channels via the bent capillaries starting from two manifold and connected to the cooling plate by four KOVAR connectors. The module is compact and can be quickly (within one weekly machine development day) replaced when the performance degradation due to the irradiation is too high ($\sim$ 100 day of data taking at the nominal intensity).

3. Performances

The standalone computation of the GTK time-stamp resolution, obtained comparing the time-stamp differences among the three stations for the same K^+ event, leads to a time-resolution of $\sim 130\,\mathrm{ns}$ for each station (Fig. 6(a)). This resolution increases over time reaching a value lower than $160\,\mathrm{ps}$ after an average fluence of $0.26 \times 10^{14}\ 1\,\mathrm{MeV}\ \mathrm{n_{eq}}/\mathrm{cm}^2$ (Fig. 6(b)). In order to investigate the relationship between the time resolution and the bias voltage applied to the sensor some measurements were made in the range $[100, 250]\,\mathrm{V}$ with $50\,\mathrm{V}$ step (the results obtained are shown in Fig. 7).

4. Conclusions

The Gigatracker was designed to be the precise beam tracker of the NA62 experiment since 2016, the first year of data taking. Its design characteristics: $0.5\%\ X_0$ of material budget per module crossed by the $75\,\mathrm{GeV}$ beam with a particle rate of $750\,\mathrm{MHz}$, a $\sim\ 130\,\mathrm{ps}$ pixel time resolution measured on each of the three stations, a momentum and angular resolution of respectively 0.2% and $16\,\mu\mathrm{rad}$, allow the detection of the first signal candidate in NA62 dataset collected in 2016 (See [9] for details on the analysis criteria, event selection and reconstruction strategies). Furthermore, because of the yearly high particle fluence ($2{\times}10^{14}\ 1\,\mathrm{MeV}\ \mathrm{n_{eq}}/\mathrm{cm}^2$), the detector was designed to be quickly (within one SPS machine development day) replaceable in time before reaching an unbearable performance degradation. The analysis of the NA62 data collected during 2017 and 2018 is ongoing.

Acknowledgments

The authors are grateful to the staff of the CERN laboratory and the technical staff of participating universities and laboratories for their valuable help during the construction, installation and commissioning of the GTK detector. The present work was completed thanks to the dedication of the whole NA62 Collaboration in operating the experiment in data-taking conditions and later in providing results from the off-line data processing. The cost of the GTK and of its auxiliary systems were supported by the funding agencies of the collaborating Institutes. We are particularly indebted to: F.R.S.-FNRS (Fonds de la Recherche Scientifique - FNRS), Belgium; INFN (Istituto Nazionale di Fisica Nucleare), Italy; CERN (European Organization for Nuclear Research), Switzerland.

References

[1] E. Cortina Gil, et al., The beam and detector of the NA62 experiment at CERN, J. Instrum. 12 (05) (2017) P05025, http://dx.doi.org/10.1088/1748-0221/12/05/P05025, arXiv:1703.08501.
[2] M. Noy, et al., Characterisation of the NA62 GigaTracker end of column readout ASIC, J. Instrum. 6 (01) (2011) http://dx.doi.org/10.1088/1748-0221/6/01/c01086, C01086–C01086.
[3] G. Aglieri Rinella, et al., The TDCpix ASIC: High rate readout of hybrid pixels with Timing Resolution Better than 200 ps, in: Proceedings, 2013 IEEE Nuclear Science Symposium and Medical Imaging Conference (NSS/MIC 2013): Seoul, Korea, October 26-November 2, 2013, 2013. http://dx.doi.org/10.1109/NSSMIC.2013.6829432.
[4] A. Kluge, et al., The TDCpix readout ASIC: A 75 ps resolution timing front-end for the NA62 Gigatracker hybrid pixel detector, Nucl. Instrum. Methods Phys. Res. A 732 (2013) 511–514, http://dx.doi.org/10.1016/j.nima.2013.06.089, URL: https://doi.org/10.1016/j.nima.2013.06.089.
[5] G. Aglieri Rinella, et al., Test-beam results of a silicon pixel detector with time-over-threshold read-out having ultra-precise time resolution, J. Instrum. 10 (12) (2015) P12016, URL: http://stacks.iop.org/1748-0221/10/i=12/a=P12016.
[6] G. Aglieri Rinella, et al., The NA62 GigaTracker, Nucl. Instrum. Methods Phys. Res. A A845 (2017) 147–149, http://dx.doi.org/10.1016/j.nima.2016.06.045.
[7] G. Romagnoli, et al., Silicon micro-fluidic cooling for NA62 GTK pixel detectors, Microelectron. Eng. 145 (2015) 133–137, http://dx.doi.org/10.1016/j.mee.2015.04.006.
[8] ISOLA group, https://www.isola-group.com/wp-content/uploads/data-sheets/fr408pdf, latest visit on March 2019.
[9] R. Marchevski, et al., First search for $K^+ \to \pi^+ \nu \bar{\nu}$ using a decay-in-flight technique, Phys. Lett. B 791 (2019) 156–166, http://dx.doi.org/10.1016/j.physletb.2019.01.067, arXiv:1503.02693.